REVISTA INTERDISCIPLINAR DE PESQUISA EM ENGENHARIA

CILAMCE 2016
XXXVII IBERIAN LATIN AMERICAN CONGRESS ON COMPUTATIONAL METHODS IN ENGINEERING
BRASÍLIA - DF - BRAZIL

WOVEN FABRICS COMPUTATIONAL SIMULATION USING BEAM-TO-BEAM CONTACTS FORMULATION

Mauro Takayama Saito

Alfredo Gay Neto

mauro.saito@usp.br

alfredo.gay@usp.br

Polytechnic School at University of São Paulo

Department of Structural and Geotechnical Engineering, São Paulo, SP, Brazil

Abstract. *This paper presents the study of the woven fabric mechanical behavior using computational simulations. For that, the finite element analysis is used, where the woven weft and warps are modeled by three-dimensional beams and the interaction among them are performed by frictionless contact models. Therefore, the methodology for the woven fabrics computational simulation is developed, such as the constitution of these numerical models and computational tests techniques are presented. For it, super elliptical cross sections are considered for warp and weft textile fibers and the beam-to-beam contact formulations are assumed in the problem solution, where parametrized surfaces represent the boundaries of the beams that are candidate to contact. The result of the computational simulations is the possibility to study the textile mechanical behavior, where their properties can be obtained for woven fabrics samples under several load cases.*

Keywords: *Woven fabrics, computational simulation, beam to beam contact*

1 INTRODUCTION

This paper presents the woven fabric computational simulation, where the beam-to-beam contact formulation was considered. Geometric nonlinearities were considered in the model, since we want to experiment scenarios of large deformation. The study is performed considering the mesoscopic level, in which is taken into account the arrangement of fibers in yarns that compound a woven fabric sample to be tested, where general mechanical properties can be determined, for instance: tensile strength, bending stiffness, compression limits and torsion stiffness.

Textile materials present a complex geometric structure and, as described by Hu (2000), they are totally different from the materials commonly used in the engineering once they are inhomogeneous, lack continuity and are highly anisotropic. Furthermore, textile materials may present large strain and large displacements under low stresses, such as present nonlinear behavior. The study of mechanical properties of textile materials can be determined by experimental or theoretical methodologies or by a combination of both.

According to Hu (2004), the woven fabrics mechanics studies date from the beginning of 20^{th} century, prompted by worldwide interest in the development of airships in Germany. Remarkable success of woven mechanics theoretical studies is compiled in two books edited by Hearle et al. (1969, 1980). In addition, Kawabata Evaluation System (KES), developed by Kawabata (1980), represent the major triumph for the fabric testing, when it became possible to provide a full description of a fabric by means of several measured parameters.

The application of computational methods for the fabric mechanics studies started in 1960s, based on Hearle (1972) fundamentals theory. And according to Grishanov (2009), it has presented an important growth during the past two decades.

Using the Finite Element Method (FEM), several authors modeled fabrics by different approaches. Considering the woven fabric as a continuum model (in which the discrete microstructure is generally neglected), using properties from KES tester and a 4-node shell element, Collier (1991) developed a large deflection and small strain analysis, for example. Hu and Newton (1993) established nonlinear constitutive equations of woven fabrics under several load conditions. In contrast, fabrics can be modelled considering the yarns constitution and the interaction among them, resulting in a non-continuum model. Important and pioneer works that can be highlighted were developed by Hearle and Shananhan (1978) and Ghosh et al. (1990).

If compared to the experimental methods, the woven fabrics computational simulation is more advantageous in the following aspects: simplicity to execute tests, once sometimes mechanical properties cannot be measured easily; lower cost, due the use of expensive testing equipment in experimental tests; the tester can create some conditions that do not correspond to the real conditions in which the textile material is used; when based on a consistent theory or model, the theoretical test can be used in general applications, even including the cases when the new material is non-existing. On the other hand, an important disadvantage of computational simulation is that the solution quality is affected by assumptions or simplifications done about the problem, to make it present a valid solution, sometimes difficult to be achieved due to high nonlinearities presented.

More recent and remarkable works in fabric computational simulation using the FEM were developed by Durville (2007), that proposed an approach to model contact-friction interaction between beams in order to simulate entangled structures at scale of individual

fibers. Nilakantan et al. (2009) presented a multiscale modelling technique to simulate the impact of flexible woven fabric, using solid and shell finite elements. Zhang (2010) demonstrates a reliability analysis methodology to solve the safety issues in the structural design of fabric structures, using the finite element method formulation.

2 BEAM MODELING

Following the work from Gay Neto et al. (2013), where the geometrically-exact formulation of Timoshenko beams are applied to offshore risers' mechanics in statics, in present work, woven warp and weft fibers are modelled by the same beam formulation. Such beams show a good numerical modeling behavior when undergoing large displacements and finite rotations. The whole theory can be found in Gay Neto et al. (2013), for static analysis and Gay Neto et al. (2014) for dynamics. Recently, a more complete presentation for dynamics can be found in Gay Neto (2016). This beam element is capable to model tension, compression, shear, bending and torsion internal loads. The beam cross section kinematics is treated as a rigid body's (no warping is assumed). The model is geometrically nonlinear.

Rotations are parametrized by Rodrigues' parameters. Due the singularities present in rotation tensor related to some values of Rodrigues's parameters, an update-Lagrangian framework is used in the formulation, allowing through sequentially sub-steps in the simulation, the achievement of the large rotations in the solution with no singularities problems in rotation tensor.

The Euler rotation vector is defined as:

$$\boldsymbol{\theta} = \theta \mathbf{e}\,, \tag{1}$$

with θ the rotation magnitude and **e** the rotation direction.

The Rodrigues' rotation parameter is defined by:

$$\alpha = 2\tan(\theta/2)\,. \tag{2}$$

Rodrigues' rotation vector ($\boldsymbol{\alpha}$) is given by:

$$\boldsymbol{\alpha} = \alpha \mathbf{e} \tag{3}$$

Using the Rodrigues' parameters and considering **A** = skew ($\boldsymbol{\alpha}$), the expression for the rotation tensor **Q** is written by (see Campello et al. (2003)):

$$\mathbf{Q} = \mathbf{I} + \frac{4}{4+\alpha^2}\left(\mathbf{A} + \frac{1}{2}\mathbf{A}^2\right) \tag{4}$$

The centroid position of each cross section is defined by the vector **z**, which is superscripted by the associated configuration index. The displacement related to each cross section centroid is defined by the vector **u** (superscripted by the associated configuration index):

$$\mathbf{u}^{i+1} = \mathbf{u}^{i} + \mathbf{u}^{\Delta} \tag{5}$$

The superscript index "i" represents a quantity associated to the configuration "i", while "i+1" is related to the end of the present time-step (configuration "i+1"). Finally, "Δ" is the gap time between the configurations "i" and "i+1".

The Rodrigues' parametrization main advantage is to express the update rotations with no need to extract the rotation vector from the updated rotation tensor (see Fig. 1). Thus, since one know $\boldsymbol{\alpha}^i$ and $\boldsymbol{\alpha}^\Delta$, $\boldsymbol{\alpha}^{i+1}$ is given by Eq. (6):

$$\boldsymbol{\alpha}^{i+1} = \frac{4}{4 - \boldsymbol{\alpha}^\Delta . \boldsymbol{\alpha}^i} \left(\boldsymbol{\alpha}^\Delta + \boldsymbol{\alpha}^i + \frac{1}{2} \boldsymbol{\alpha}^\Delta \times \boldsymbol{\alpha}^i \right) \tag{6}$$

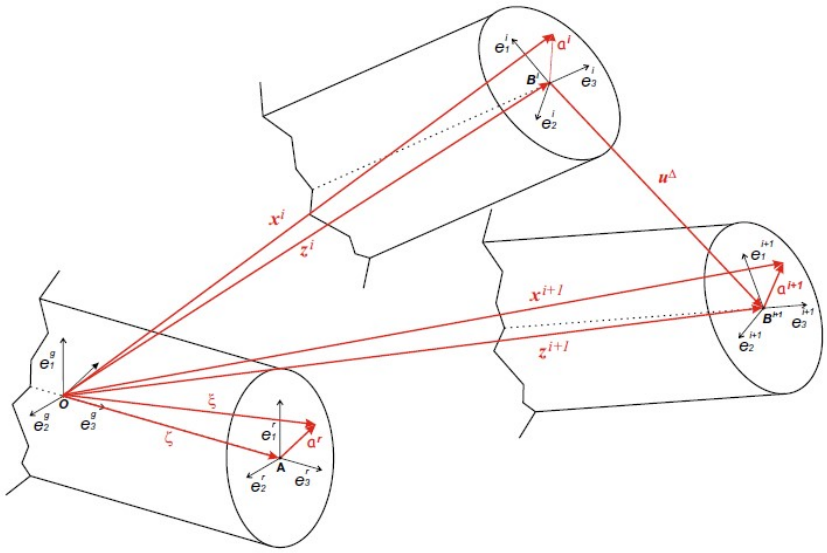

Figure 1. Beam cross section kinematics (figure from Gay Neto (2013))

Superimposed rigid body motions are considered due the large displacements and finite rotations. As done by Gay Neto (2013), the internal loads derivation is performed in the reference configuration, by backing-rotation procedures. The generalized stress considered for the beam model comes from First Piola-Kirchhoff stress tensor.

A spatial discretization considering 3-node elements and a quadratic interpolation was considered for both displacements and rotations fields. Also, isoparametric formulation was assumed, as shown by Gay Neto (2013).

3 BEAM TO BEAM CONTACT MODELING

The interaction between the initially orthogonal beam elements modeled is performed by a beam-to-beam contact formulation. The fundamentals of a pointwise contact between circular cross section beams were developed by Wriggers and Zavarise (1997), in which beam axes are parametrized as three-dimensional curves and a gap function is defined, when the minimum distance point between the curves is assessed.

The beam-to-beam contact modeling applied in this work is based on the approach for a surface-to-surface contact for super ellipses beam cross sections, where no master and slave distinction is done. According to Gay Neto et al. (2016), the surfaces considered for a contact pair are parameterized by convective coordinates (used to map the material points along the surfaces) and they receive the same treatment (no slave points are considered), characterizing this way the master-surface to master-surface formulation approach.

Then, the material node points of contact surfaces are defined by the minimum distance problem solution, using the local optimization problem concept. The master-surface to master-surface contact formulation presents less computational effort if compared to the other methods, because for each pair of surfaces, only a single gap is evaluated.

Also, an important aspect considered in the approach of this contact formulation is the distributed load representation by a pointwise mechanical equivalent load. Then, scenarios with non-pointwise contact interaction may be modeled increasing the discretization of beam surfaces in more surface pairs leading to more pointwise interactions in the contact between two beams and results will reflect a more realistic behavior in the surfaces contact.

Some formulation limitations need to be highlighted, for instance, the dealing with non-convexity of the minimum distance problem. It occurs when two parallel planes are considered and several possible approaches can be used in the choice for the discretization of multiple pointwise contact actions. An example for the beam-to-beam contact context is the contact between two parallel beams that cannot be solved directly and needs special treatments.

Figure 2 shows two generic bodies (A and B), that are candidate to the contact and the gap function **g**, for which the minimum distance problem between the surface body surfaces needs to be evaluated.

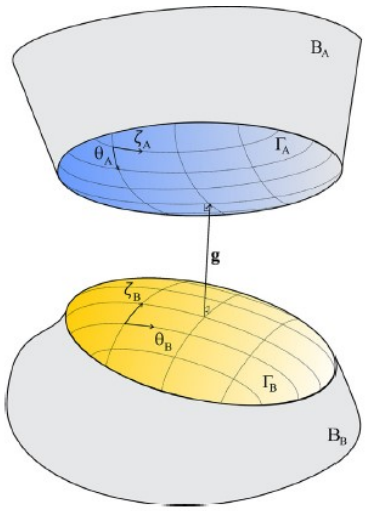

Figure 2. Bodies A and B candidates to contact interaction (Figure from Gay Neto (2016))

4 GIRAFFE PLATFORM

The finite element method platform to perform the woven fabric simulations is named *Giraffe* (*Generic Interface Readily Accessible for Finite Elements*), developed on a C++ code. It is a generic platform, on which it is possible solve several structural models using different degrees of freedom.

Giraffe platform was started by Gay Neto (2014) in Polytechnic School at University of São Paulo. It already includes a geometrically-exact beam element for simulations that present geometric nonlinearities and beam-to-beam contact formulations, previously presented in this paper.

5 WOVEN FABRICS COMPUTATIONAL SIMULATION

Using the *Giraffe* platform, a woven fabric sample computational simulation can be performed. This problem is highly geometric-nonlinear, once large displacements and finite rotations of yarns are expected, as well as the nonlinear mechanical contact behavior between the weft and warp fibers.

In order to achieve the numerical model convergence, some adoptions were established for the woven fabrics simulation. Both static and dynamic computational simulations approaches were sequentially performed, in which, for the first of them, the woven fabric geometry and mesh are constituted. Also, the initial boundary conditions are applied to the model, in order to establish the main characteristics of fabric sample.

The dynamic solution is performed to solve the mechanical computational tests of woven fabrics, where forces and/or displacements are applied to the model. Dynamic solution was adopted due its greater robustness if compared to the static solution. The modeling of mechanical contact nonlinear behavior between the weft and warps fibers under displacements or forces leads to abrupt stiffness changes and this mechanical aspect demanded the choice for more robust solution method. For the model solution, arc-length method could be used in a static approach as an alternative, however dynamics was chosen due to the more realistic behavior.

5.1 Static Analysis

The static analysis approach consists in the fabric meshing constitution before the mechanical tests. First, the geometric and mechanical properties for weft and warp yarns of woven fabric sample are set, as follows:

- Number of weft/warp yarns;
- Weft/warp yarns length;
- Number of elements along weft/warp yarns length;
- Material Young Moduli;
- Material Poisson ratios;
- Material densities;
- Semi axis "*a*" of superellipse beam cross section;
- Semi axis "*b*" of superellipse beam cross section;
- Exponent "n" of superellipse beam cross section;
- Discretization in Finite Difference Method of superellipse for Saint Venant Torsion calculation;
- Friction coefficient;
- Normal penalty parameter;
- Tangential penalty parameter;
- Pinball radius;

In the Cartesian system of coordinates, the superellipse cross section boundary curve is shown in Eq. (7):

$$\left|\frac{x}{a}\right|^n + \left|\frac{y}{b}\right|^n = 1 \tag{7}$$

The static analysis is divided into four load steps, as described as follows:

Load Step 0. This is the initial woven fabric geometry constitution in a 2D plane, which there is no real geometry correspondence. The number of wefts and warps are defined for the computational woven sample, as well as their lengths and the element sizes. Wefts and warps fibers are set in a plane, where they intercept geometrically each other. However, no interaction (contact) between the orthogonal beams is predicted, only the initial position of woven yarns is set.

Load Step 1. There is an initial displacement imposition, opening the warp fibers regarding the weft fibers that remain at initial configuration displacement. The warp node displacements are set so that there is a small gap between the orthogonal weft and warp cross sections. At this load step, no interaction or contact between the warp and weft fibers is established. Only node displacements are input.

Load Step 2. There is a displacements imposition, in order to achieve an initial contact between the orthogonal fibers. However, this step is more critical than the previous one, once the beam to beam contact is set by the first time.

Load Step 3. Release the displacements previously set, allowing the system to reach a neutral condition. The six degrees of freedom of each node are released, in exception for the border nodes (boundaries of the considered fabric specimen).

Load Step 4. Degrees of freedom restrains are set at the sample woven fabric borders. This load step is important to boundary conditions settings of specific mechanical tests.

5.2 Dynamic Analysis

In sequence to the woven fabric constitution through all static analysis load steps, the computational mechanical test can be effectively done performing the dynamic transient nonlinear analysis.

In Giraffe platform, Newmark method is used to integrate displacements along time, in which two coefficients β equal to 0.3 and γ equal 0.5 are defined and recommended to result in a time-integration without numerical damping relevance. The method application is more explained by Gay Neto (2016), which reference is Ibrahimbegovic (1998).

Among some parameters to be set for the dynamic analysis, the damping control must be commented, once the results convergence is closely dependent on this aspect. In *Giraffe*, Rayleigh damping model is implemented, in which two attribute constants are set: α and β coefficients, as shown in Eq. (1):

$$C = \alpha.\mathbf{M} + \beta.\mathbf{K} \tag{1}$$

In which α is the mass proportional damping coefficient, β is the stiffness proportional damping coefficient, **M** is the mass matrix, **K** is the stiffness matrix and **C** is the resultant damping matrix.

6 NUMERICAL SIMULATION

In this section, a numerical methodology and results examples are presented. It was considered a woven fabric sample 3 by 3: composed by three warps (parallel to x axis) and three wefts (parallel to y axis), as shown in the Fig. 3(a). The beam elements are shown rendered as solids, permitting the beam external surfaces and the beam-to-beam contact realistic visualization. Also, are shown the adopted global coordinate system and the identification A-B-C-D sample borders. All the post-processing figures were obtained using the open source Paraview® software.

The material mechanical properties are based on the Polyamide 6 (PA6). They are shown in the Table 1. Subscripted index i equal to 1 corresponds to weft yarns and 2 to warp yarns properties.

Table 1. Model data

Properties	Symbol [unit]	Weft yarn	Warp yarn
Quantity	N_i [ ]	3	3
Length	L_i [m]	0.50	0.50
Elements along length	M_i [ ]	31	31
Young Modulus	E_i [Pa]	2.40E+09	2.40E+09
Poisson ratio	ν_i [ ]	0.39	0.39
Density	ρ_i [kg/m³]	11300	11300
Superellipse semi axis "*a*"	r_{Ai}[m]	0.025	0.025
Superellipse semi axis "*b*"	r_{Bi} [m]	0.025	0.025
Superellipse exponent	ni [ ]	2.00	2.00
Discretization for TSV	FDM_i [ ]	100	100
Normal penalty parameter	EPN_i [ ]	1.00E+08	1.00E+08
Tangential penalty parameter	EPTi [ ]	1.00E+07	1.00E+07
Friction coefficient	MU_i [ ]	0.00	0.00
Pinball radius	PB_i [m]	0.10	0.10

Friction coefficient was considered null in this example. In order to get an easier convergence solution, the application of a Rayleigh damping was necessary. Damping coefficient must be enough to guarantee the numerical convergence and not affect the

mechanical results substantially. If one sets a large damping, the model dissipates excessive energy. On the other hand, if one sets a too low damping, high frequency numerical vibration modes can be excited and it leads to a divergent solution. For the numerical example calibration, the following Rayleigh stiffness proportional coefficient damping β were applied for different computational tests shown in the Table 2.

Table 2. Stiffness proportional coefficient damping β

Computational test	β
1	0.3
2	0.03
3	0.003
4	0.0003

6.1 Static Analysis

Load Step 0. Figure 3(a) shows bi-dimensional plane woven fabric constitution. In the example, a 3 by 3 yarns example is shown in a rendered visualization. Woven yarns align to x-axis (red) are the weft fibers and yarns parallel to y-axis (yellow) are the warp fibers.

Load Step 1. The displacements imposition is applied to the model, where the warp fibers are opened around the weft fibers (Fig. 1(b)). The weft fibers remain at the initial position. At borders, all translational degrees of freedom are set zero. Rotational degrees of freedom at x and y axis are set free. At z-axis, rotation is set null. Only one sub step is necessary, once displacements are applied to the warp nodes.

a b

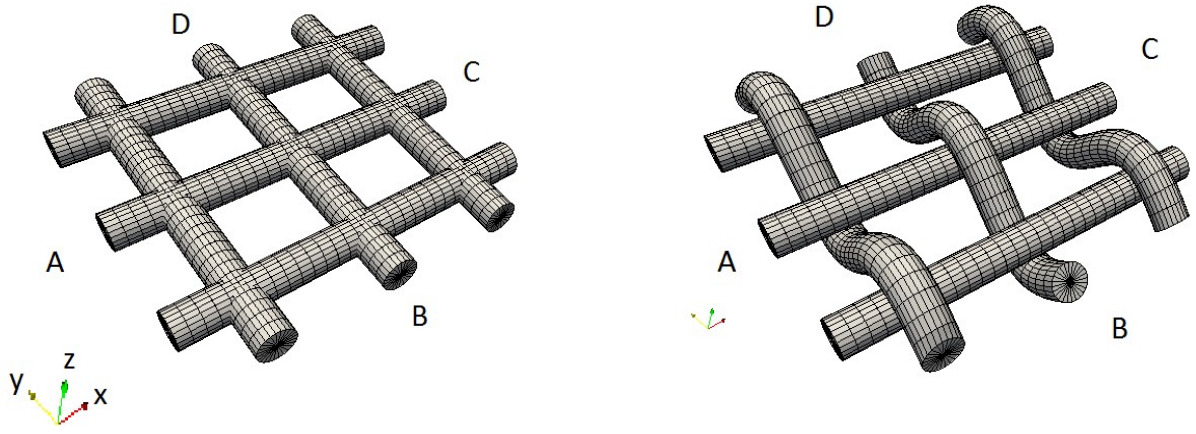

Figure 3. (a) 2D plane woven fabric constitution; (b) Warp fibers opening

Load Step 2. After imposing new displacements at weft fibers, they reach an initial contact with warp fibers, as shown in Fig. 4(a). Ten sub steps are set for this load step, once initial contacts between the fibers are established at this load step and high nonlinearities are present.

Load Step 3. Figure 4(b) shows the woven fabric sample neutral condition, in which the degrees of freedom are set free, except for the borders, where all translational degrees of freedom are set zero and axis z rotation is zero, too.

Load Step 4. Degrees of freedom restrains are set for sample woven fabric borders. This load step is important to boundary conditions settings of specific mechanical tests.

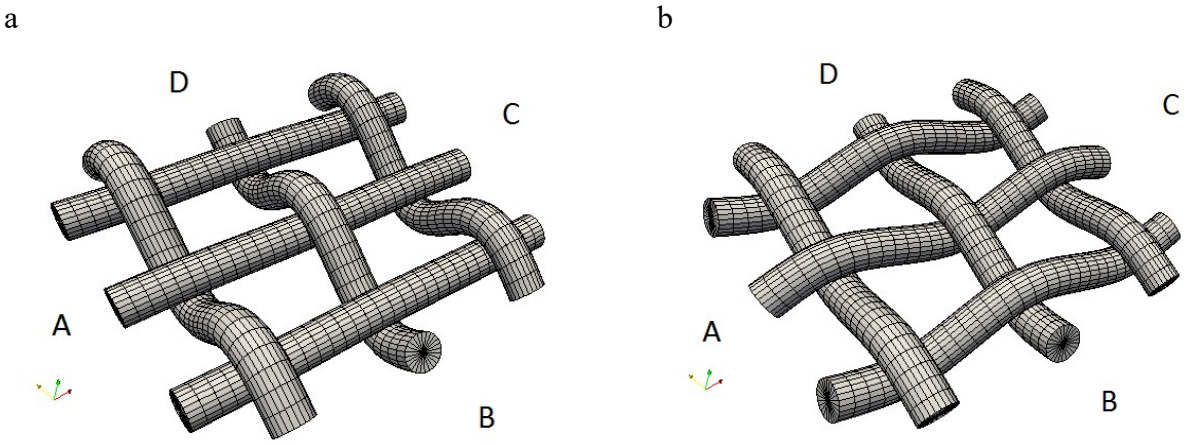

Figure 4. (a) Initial contact between warp and weft fibers; (b) Neutral condition

6.2 Dynamic Analysis

The transient analysis consists in the displacement prescription at the three nodes of C border at positive x axis direction, as presented in the diagram at Fig. 6.

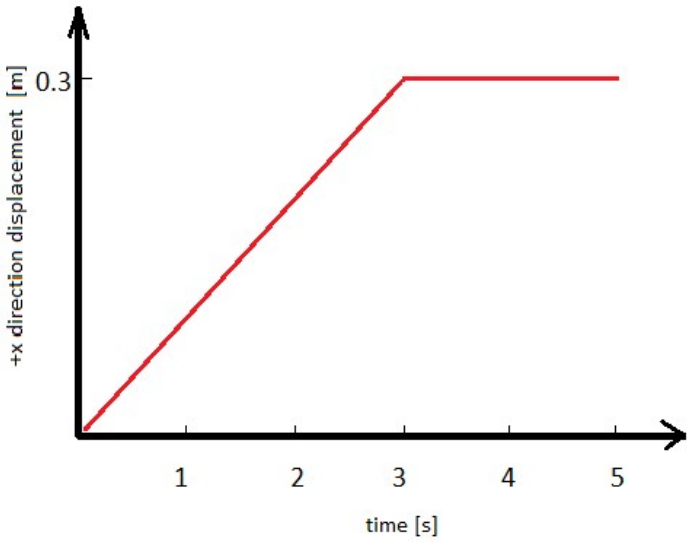

Figure 5. Displacement at border C nodes versus time

During 3 seconds, it is applied a constant displacement gradient at C border nodes. After, the final position achieved is kept for 2 seconds (0.3 m). This allows the system to achieve the equilibrium after the displacements imposition (neutral condition).

Figure 6 (a – d) show the initial, intermediate and final rendering visualizations for the dynamic analysis test considering the stiffness proportional coefficient damping β equal to 0.003 (computational test 3).

a b

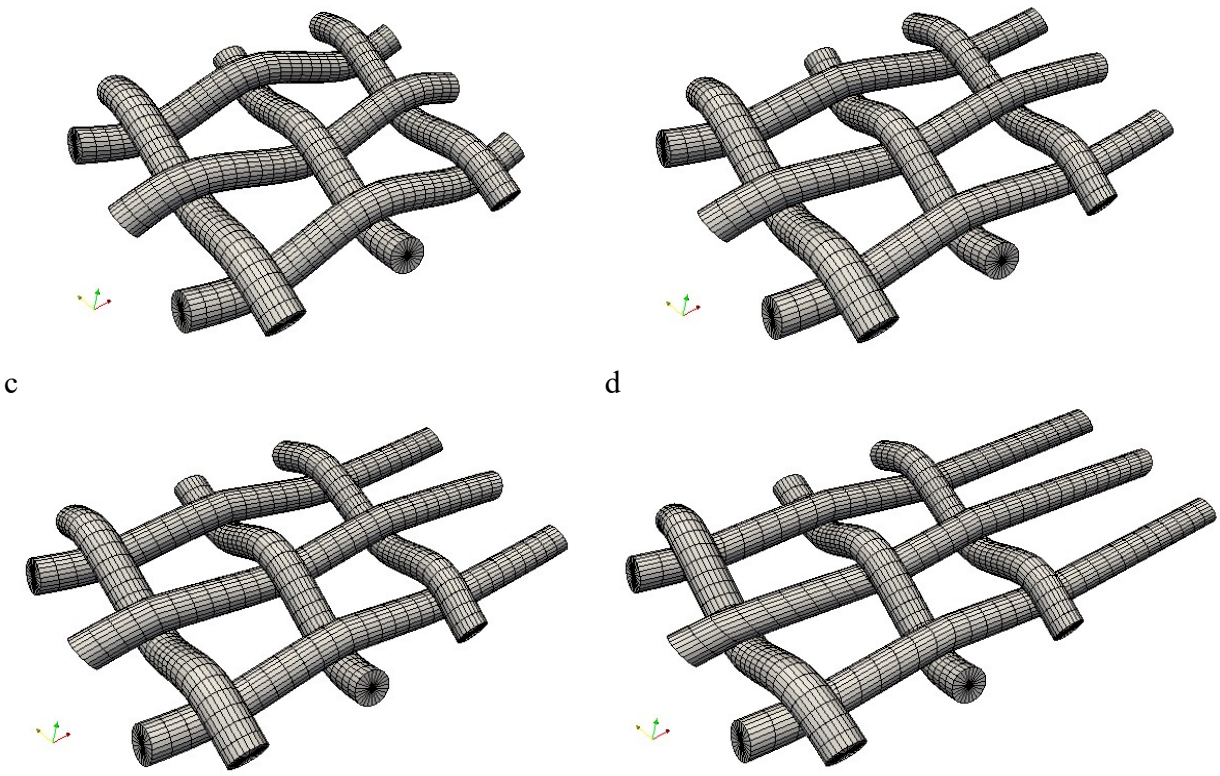

c d

Figure 6. Rendering visualization for dynamic analysis (a) Time step 0s; (b) Time step 1.111s; (c) Time step 2.778s; (d) Time step 5 .000 s

The following diagrams (Fig. 7 to 10) show the forces reactions for each woven border sample during the time. Each curve represents a different proportional stiffness coefficient β, identified according to the diagrams labels. For the computational tests 1 and 2 (β equal to 0.3 and 0.03, respectively), a notable difference in reaction forces could be observed if compared to the lower β, considered in computational tests 3 and 4. This means that for the Rayleigh coefficients considered in the computational tests 1 and 2, excessive energy is dissipated and it influences in the mechanical behavior of the model.

For the computational tests 3 and 4, the reaction forces are very similar if compared to each other, indicating a convergence in results for the adopted damping coefficients. Once lower values for β lead to more expensive computational costs or even divergent solution, the most suitable proportional stiffness damping coefficient is that applied to computational test 3 (β = 0.003).

An important remark is about the computational test 1 convergence results, for which is possible to observe a known and unwished behavior in the contact between the warp and weft fibers – excessive time steps and bisections to converge the model. It occurs due non-continuity between the adjacent elements parametrization surfaces in the model. This issue is discussed by Gay Neto et. al. (2016).

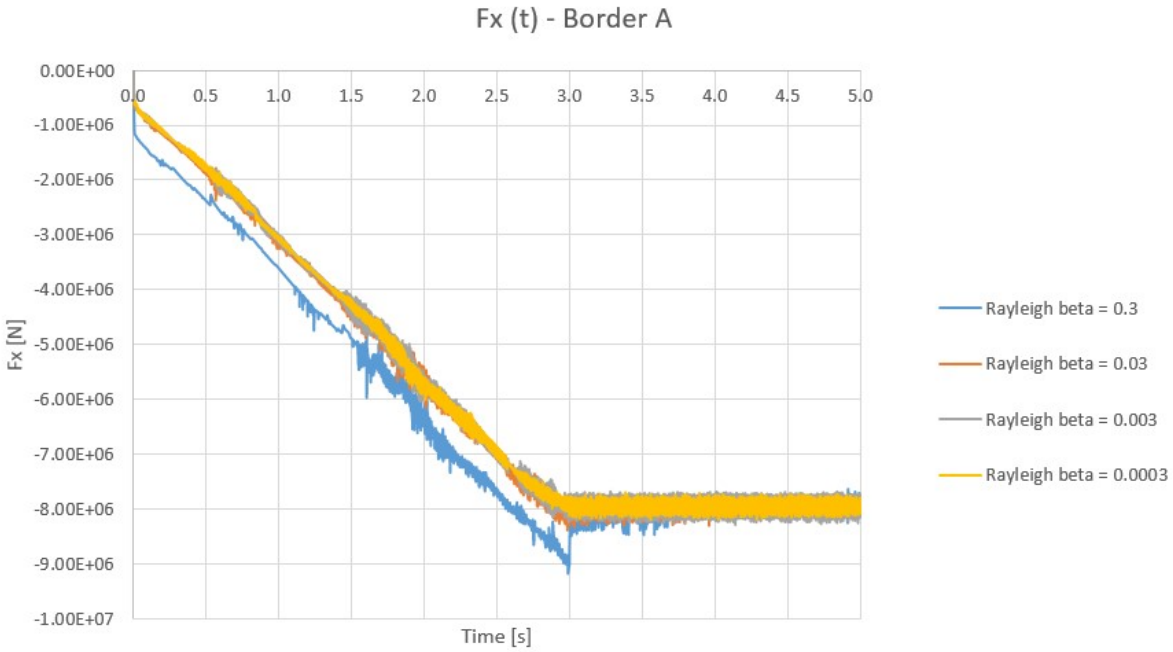

Figure 7. Force Reaction (x direction) in the border A

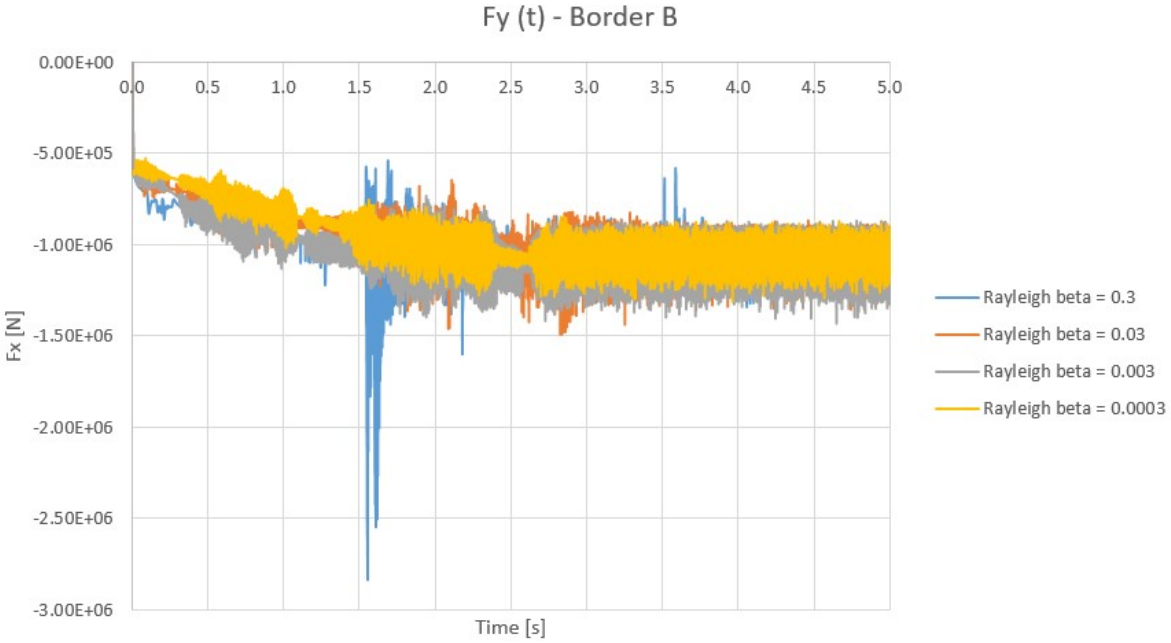

Figure 8. Force Reaction (y direction) in the border B

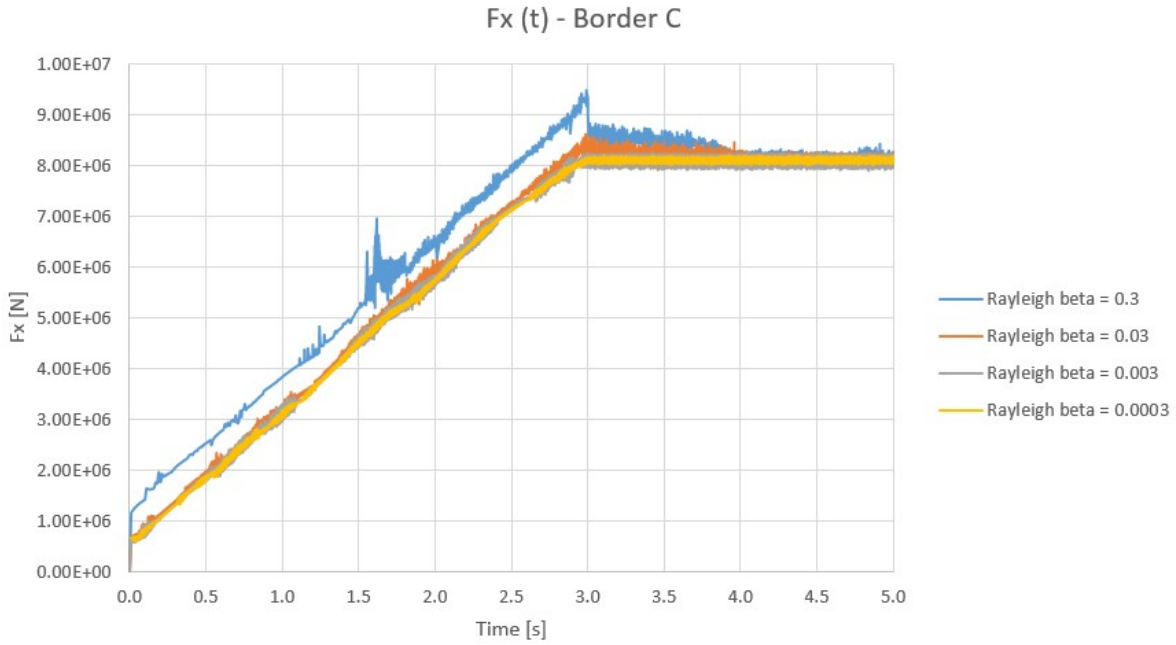

Figure 9. Force Reaction (x direction) in the border C

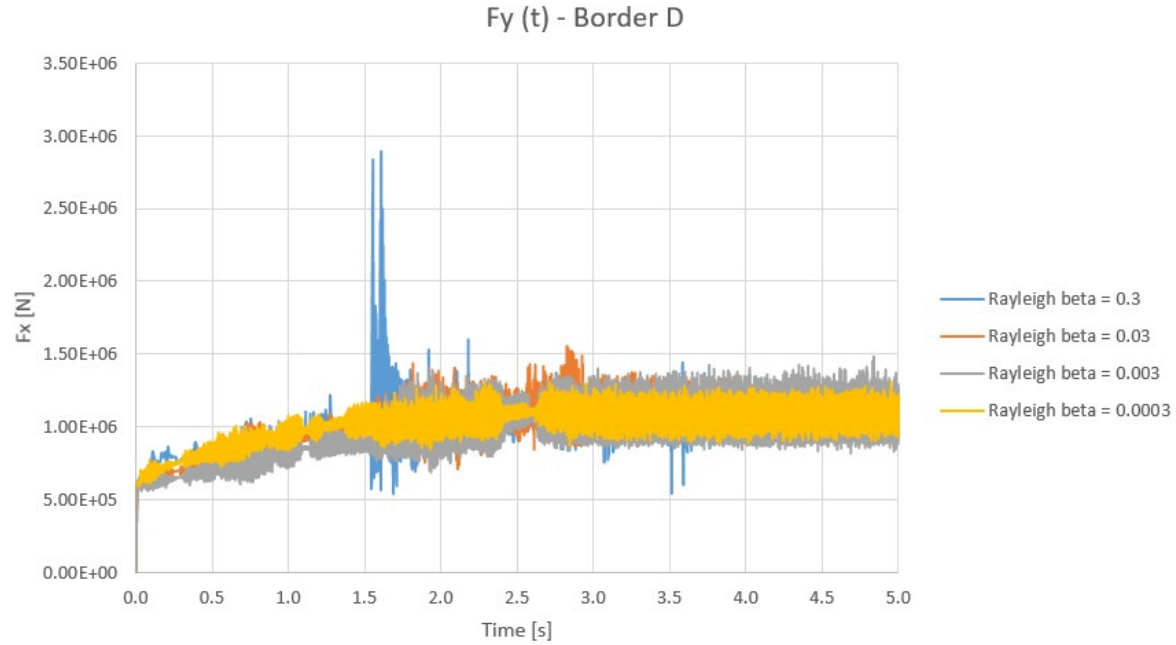

Figure 10. Force Reaction (y direction) in the border D

The internal loads can also be analyzed to verify the mechanical behavior of the model. Relevant results, as shear and axial forces, can be plotted for the rendering visualization in Paraview® software, as shown in Fig. 11 and Fig. 12. The maximum normal forces at final time step occur in the tension warp fibers nearby the border C region, when displacements are applied to the model. The maximum shear forces are observed on the elements of warp tensioned fibers, close to the contact between the orthogonal weft fibers.

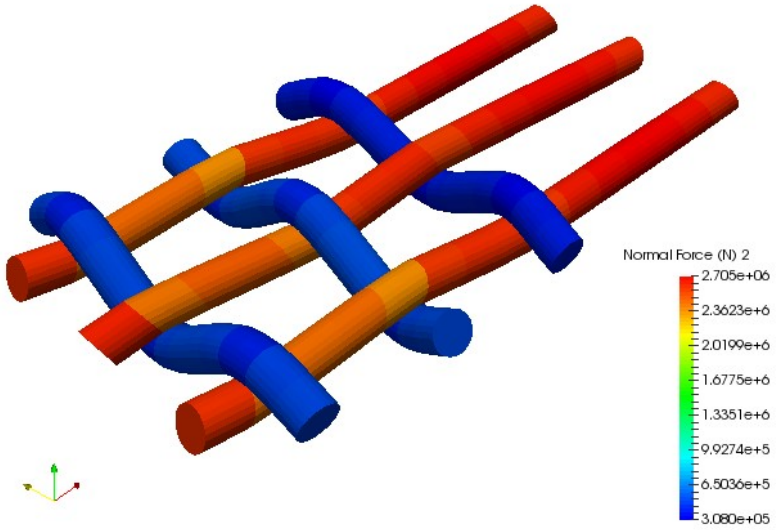

Figure 11. Normal Forces plotting for computational test 3 – Time step: 5 s

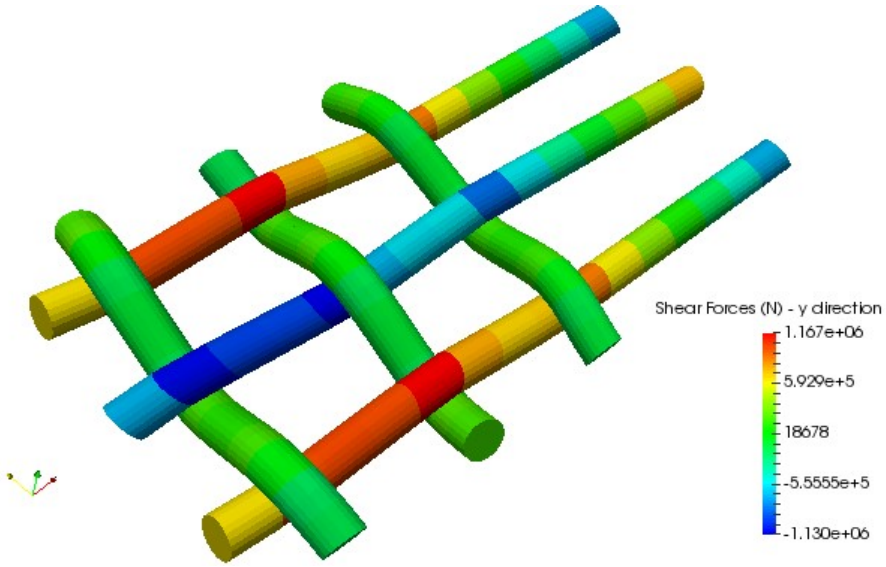

Figure 12. Shear forces at y direction plotting for computational test 3 – Time step: 5 s

Figure 13 shows the detail of the realistic contact rendering visualization between the warp and weft fibers. An important parameter to achieve reasonable penetration values between the fibers is the penalty parameter (shown in Table 1). Penalty parameter value was chosen based on the classical Hertz contact theory, considering the idealized model of two cylinders in contact and lie on perpendicular axes, as proposed by Popov (2010). Once contact friction set in the model is zero, even though is presented in the Table 1, tangential penalty parameter is not considered in the frictionless contact formulation.

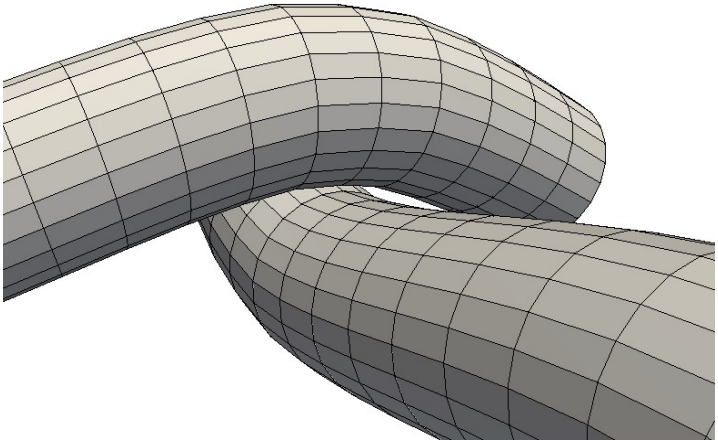

Figure 13. Detailed contact visualization

7 CONCLUSION

In this work it was proposed the methodology for the study of woven fabric mechanical behavior using the Finite Element Method, considering the beam-to-beam contact formulation. Mechanical fabrics concepts present an extensive theoretical knowledge and the application of them in numerical models using computational simulations has obtained success and has become a trend to new textile materials development, mechanical interaction of fibers study etc.

The methodology purposed for the numerical example showed a good performance for the complexity contact interactions involved in the dynamic solution. The obtained results of computational simulation achieved the expected results, once the presented numerical example showed in this work required critical conditions to the convergence solution, even though the present model had a reduced size.

As continuity of this work, the friction between the textile fibers will be implemented in the model and new calibration parameters will be necessary to achieve the convergence for the numerical model. Also, an automatic mesh generator is being developed for different woven fabrics patterns constitution.

8 ACKNOWLEDGEMENTS

The second author acknowledges the support from CNPq (Conselho Nacional de Desenvolvimento Científico e Tecnológico) under the grant 308190/2015-7.

REFERENCES

Collier, J. R., Collier, B. J., Toole, G. O. & Sargrand, S. M., 1991, *Drape prediction by meansof finite element analysis*, J Text Inst, 82(I), 96–107.

Durville, D., 2011. Contact Modelling in Entangled Fibrous Materials. In Zavarise, G & Wriggers, P, eds, *Trends in Computational Contact Mechanics*, pp. 1- 22. Springer-Verlag.

Durville, D., 2007. Finite element simulation of textile materials at mesoscopic scale. *Finite element modelling of textiles and textile composites*, pp. CDROM <hal-0027046>.

Gay Neto, A., C. A. Martins, & P. M. Pimenta. Static analysis of offshore risers with a geometrically-exact 3D beam model subjected to unilateral contact. *Computational Mechanics*, v. 53, 2014: 125-145.

Gay Neto, A., 2016. Dynamics of offshore risers using a geometrically-exact beam model with hydrodynamic loads and contact with the seabed. *Engineering Structures*, v. 125:438-454

Gay Neto, A., & C. A. Martins, 2013. Structural stability of flexible lines in catenary configuration under torsion. *Marine Structures*, v. 34: 16-40.

Gay Neto, A., P. M. Pimenta, e P. Wriggers., 2014. Contact between rolling beam and flat surfaces. *International Journal for numerical Methods in Engineering,* v. 97:683-706.

Gay Neto, A., P. M. Pimenta, e P. Wriggers, 2014. Self-contact modeling on beams experiencing loop formation. *Computational Mechanics*, v. 55, 2014: 193-208.

Gay Neto, et. al., 2016. A master-surface to master-surface formulation for beam to beam contact. Part I: frictionless interaction. *Computer Methods in Applied Mechanics and Engineering*.

Gay Neto, A. The Giraffe Project. 2014. http://sites.poli.usp.br/p/alfredo.gay/ (accessed in July 15th, 2016).

Ghosh, T. K., Batra, S. K. & Barker, R. L., 1990. *Bending behaviour of plain-woven fabrics: a critical review*, J Text Inst, 81, 245–287.

Grishanov, S., Fundamental Modelling of Textile Fibrous Structures. In Chen, X.,2010. *Modelling and Predicting Textile Behavior*, CRC Press.

Hearle, J.W.S., Grosberg, P., & S. Baker., 1969. *Structural Mechanics of Fibers, Yarns, & Fabrics*, Vol. 1, John Wiley& Sons.

Hearle, J. W. S., Thwaites, J. J. & Amirbayat, J., 1980. Mechanics of Flexible Fiber Assemblies. *NATO Advanced Study Institute Series*: E, Applied Sciences No. 38.

Hearle, J. W. S., Konopasek, M. & Newton, A., 1972. *On some general features of a computer-based system for calculation of the mechanics of textile structures*, Text Res J, 10, 613–626.

Hearle, J. W. S. & Shanahan, W. J., 1978. *An energy method for calculations in fabric mechanics, Part I: Principles of the method*, J Text Inst, 69, 81–91.

Hu, J., 2004. Structure and mechanics of woven fabrics. Woodhead Publishing.

Hu, J. & Newton, A., 1993. *Modelling of tensile stress-strain curves of woven fabrics*, J China Text Univ, 10(4), 49–61.

Ibrahimbegovic, A. & Mikdad, M. A., 1998. Finite Rotations in Dynamics of beams and implicit time stepping schemes. *International Journal for Num. Methods In Engineering*., V. 41, 781-814, 1998.

Kawabata, S., 1980. *Standardization and Analysis of Hand Evaluation*. Textile Machinery Society of Japan.

Morton, W.E. & Hearle, J. W. S., 2008. *Physical Properties of Textile Fibers*. Woodhead Publishing

Nilakantan, G., Keefe, M., Bogetti, T., Adkinson, R., Gillespie Jr., J., 2009. On the finite element analysis of woven impact multiscale modeling techniques. *International Journal of Solid and Structures 47,* 2300-2315.

Popov, V.L., 2010. *Contact Mechanics and Friction.* Springer.

Zavarise, G., Wriggers, P. *Trends in Computational Contact Mechanics*. Springer, 2011.

Zhang, L., 2010. *Reliability Analysis of Fabric Structures*. Doctoral Thesis, Newcastle University.